Conformational Equilibrium Isotope Effects in Glucose by ^{13}C NMR Spectroscopy and Computational Studies†

Brett E. Lewis and Vern L. Schramm*,‡

Contribution from the Department of Biochemistry, Albert Einstein College of Medicine, 1300 Morris Park Avenue, Bronx, New York 10461

Received September 6, 2000. Revised Manuscript Received November 15, 2000

Abstract: Anomeric equilibrium isotope effects for dissolved sugars are required preludes to understanding isotope effects for these molecules bound to enzymes. This paper presents a full molecule study of the α- and β-anomeric forms of D-glucopyranose in water using deuterium conformational equilibrium isotope effects (CEIE). Using 1D ^{13}C NMR, we have found deuterium isotope effects of 1.043 ± 0.004, 1.027 ± 0.005, 1.027 ± 0.004, 1.001 ± 0.003, 1.036 ± 0.004, and 0.998 ± 0.004 on the equilibrium constant, $^{H/D}K_{\beta/\alpha}$, in [1-^{2}H]-, [2-^{2}H]-, [3-^{2}H]-, [4-^{2}H]-, [5-^{2}H]-, and [6,6′-$^2H_2$]-labeled sugars, respectively. A computational study of the anomeric equilibrium in glucose using semiempirical and *ab initio* methods yields values that correlate well with experiment. Natural bond orbital (NBO) analysis of glucose and dihedral rotational equilibrium isotope effects in 2-propanol strongly imply a hyperconjugative mechanism for the isotope effects at H1 and H2. We conclude that the isotope effect at H1 is due to $n_p \rightarrow \sigma^*$ hyperconjugative transfer from O5 to the axial C1−H1 bond in β-glucose, while this transfer makes no contribution to the isotope effect at H5. The isotope effect at H2 is due to rotational restriction of OH2 at 160° in the α form and 60° in the β-sugar, with concomitant differences in $n \rightarrow \sigma^*$ hyperconjugative transfer from O2 to CH2. The isotope effects on H3 and H5 result primarily from syn-diaxial steric repulsion between these and the axial anomeric hydroxyl oxygen in α-glucose. Therefore, intramolecular effects play an important role in isotopic perturbation of the anomeric equilibrium. The possible role of intermolecular effects is discussed in the context of recent molecular dynamics studies on aqueous glucose.

Introduction

Sugars are found as an important part of most aspects of cellular structure and energy utilization. Nucleic acids, lectins, most extracellular eukaryotic proteins and the substrates of glycolysis, the pentose phosphate pathways, and others require some participation by carbohydrate. The important roles of sugars in biology have led to theoretical and experimental investigations to understand the factors that affect their conformations, relative rotamer stabilities, and anomeric abundances. The anomeric effect, first proposed by Lemieux[1] and arguably the most significant energetic stabilizing factor in sugar chemistry, has been studied extensively in sugars and smaller molecules both experimentally[2−5] and theoretically.[6−15] While the anomeric effect may be the most discussed aspect of sugar chemistry, it is by no means the only determinant of molecular structure and energy. In fact, carbohydrates are complicated molecules, and a number of experimental and theoretical techniques have been brought to bear on their total molecular structure and behavior. Raman and infrared spectroscopic studies have been used to assign vibrational bands to specific bond stretches, angle bends, and coupled motions.[16−22] NMR studies of glucose have been able to demonstrate differences in extracyclic hydroxymethyl rotamer populations between the α- and β-pyranose anomers,[23] and a variety of chemical shift and coupling constant data have been reported.[24−32] Most recently,

† Supported by research grant GM41916 from the National Institutes of Health.

‡ Telephone (718) 430-2813. Fax (718) 430-8565. E-mail vern@aecom.yu.edu.

(1) Lemieux, R. U.; Chu, N. J. *Abstracts of Papers, Am. Chem. Soc*. **1958**, *133*, 31N.
(2) Hamlow, H. P.; Okuda, S. *Tetrahedron Lett*. **1964**, *37*, 2553−9.
(3) Bailey, W. F.; Rivera, A. D.; Rossi, K. *Tetrahedron Lett*. **1988**, *29*, 5621−4.
(4) Weisman, G. R.; Johnson, V. B.; Coolidge, M. B. *Tetrahedron Lett*. **1981**, *22*, 4365−8.
(5) McKean, D. C. *Chem. Soc. Rev*. **1978**, *7*, 399−422.
(6) Wolfe, S.; Pinto, B. M.; Varma, V.; Leung, R. Y. N. *Can. J. Chem*. **1990**, *68*, 1051−62.
(7) Salzner, U.; von Ragué Schleyer, P. *J. Am. Chem. Soc*. **1993**, *115*, 10231−6.
(8) Jeffrey, G. A.; Pople, J. A.; Radom, L. *Carbohyd. Res.* **1972**, *25*, 117−31.
(9) Jeffrey, G. A.; Pople, J. A.; Binkley, J. S.; Vishveshwara, S. *J. Am. Chem. Soc*. **1978**, *100*, 373−9.
(10) Cramer, C. J. *J. Org. Chem.* **1992**, *57*, 7034−43.
(11) Wolfe, S.; Kim, C.-K. *Can. J. Chem*. **1991**, *69*, 1408−12.
(12) Alabugin, I. V. *J. Org. Chem*. **2000**, *65*, 3910−3919.
(13) Anderson, J. E. *J. Org. Chem*. **2000**, *65*, 748−54.
(14) Wolfe, S.; Whango, M.-H.; Mitchell, D. J. *Carbohyd. Res.* **1979**, *69*, 1−26.
(15) Salzner, U.; von Ragué, S.; P. *J. Org. Chem*. **1994**, *59*, 2138−55.
(16) Bell, A. F.; Barron, L. D.; Hecht, L. *Carbohyd. Res*. **1994**, *257*, 11−24.
(17) Wen, Z. Q.; Barron, L. D.; Hecht, L. *J. Am. Chem. Soc*. **1993**, *115*, 285−92.
(18) Wang, Y.; Tominaga, Y. *J. Chem. Phys*. **1994**, *100*, 2407−12.
(19) Vasko, P. D.; Blackwell, J.; Koenig, J. L. *Carbohyd. Res.* **1971**, *19*, 297−310.
(20) Vasko, P. D.; Blackwell, J.; Koenig, J. L. *Carbohyd. Res.* **1972**, *23*, 407−16.
(21) Longhi, G.; Zerbi, G.; Paterlini, G.; Ricard, L.; Abbate, S. *Carbohyd. Res.* **1987**, *161*, 1−22.
(22) Mathlouthi, M.; Luu, D. V. *Carbohyd. Res*. **1980**, *81*, 203−12.
(23) Nishida, Y.; Ohrui, H.; Meguro, H. *Tetrahedron Lett.* **1984**, *25*, 1575−8.
(24) Forrest, T. P. *Can. J. Chem*. **1974**, *52*, 4095−100.
(25) Bock, K.; Lundt, I.; Pedersen, C. *Tetrahedron Lett*. **1973**, *13*, 1037−40.

10.1021/ja003291k CCC: $20.00 © 2001 American Chemical Society
Published on Web 01/24/2001

empirical relationships between homo- and heteronuclear coupling constants and carbohydrate conformation[24,33−38] and several *ab initio*[39,40] and molecular dynamics[41−43] studies have been used to explain the relative free energies of glucose anomers and their rotamers.

Latitudinally, conformational equilibrium isotope effects have been used to study molecular structure in a large number of compounds. Methylpyridines,[44,45] 1,3-dioxanes,[46] 3-azabicyclo-[3.2.2]nonanes,[47] and cyclohexane derivates[48−51] can each serve as simple models for carbohydrates. In fact, hyperconjugation and steric interactions contribute to equilibrium isotope effects in these molecules in a well-understood way. However, whereas previous studies employed singly substituted molecules to analyze individual effects, no study to our knowledge has been carried out on multiple substitutions in a single molecule to demonstrate the interaction of effects. This has provided an opportunity to explore the complete structure of glucose, the central carbohydrate of biology, with a probe as well understood as conformational equilibrium isotope effects.

First we report complete data for the deuterium isotope effects on the anomeric equilibrium of D-glucose in water. Then we present conformational ensembles which are most likely to compose these anomers in solution and which confirm the experimental isotope effects. On the basis of these models and calculations using gas-phase 2-propanol and methane, we are able to explain these isotope effects in the context of the anomeric effect, hydroxyl rotational restriction, and syn-diaxial steric repulsion. These results are also discussed in terms of some recent theoretical studies.

(26) Cussans, N. J.; Huckerby, T. N. *Tetrahedron* **1975**, *31*, 2719−26.
(27) Bock, K.; Pedersen, C. *J. Chem. Soc., Perkin Trans. 2* **1974**, 293−7.
(28) Bock, K.; Thogersen, H. *Ann. Rep. NMR Spec.* **1982**, *13*, 37−41.
(29) Schwarcz, J. A.; Perlin, A. S. *Can. J. Chem.* **1972**, *50*, 3667−76.
(30) Perlin, A. S.; Casu, B. *Tetrahedron Lett.* **1969**, *34*, 2921−4.
(31) Bock, K.; Pedersen, C. *Acta Chem. Scand.* **1975**, *B 29*, 258−64.
(32) Walker, T. E.; London, R. E.; Whaley, T. W.; Barker, R.; Matwiyoff, N. A. *J. Am. Chem. Soc.* **1976**, *98*, 5807−13.
(33) Serianni, A. S.; Wu, J.; Carmichael, I. *J. Am. Chem. Soc.* **1995**, *117*, 8645−50.
(34) Serianni, A. S.; Bondo, P. B.; Zajicek, J. *J. Magn. Reson., Ser. B* **1996**, *112*, 69−74.
(35) Zhao, S.; Bondo, G.; Zajicek, J.; Serianni, A. S. *Carbohyd. Res.* **1998**, *309*, 145−52.
(36) Church, T.; Carmichael, I.; Serianni, A. S. *Carbohyd. Res.* **1996**, *280*, 177−186.
(37) Carmichael, I.; Chipman, D. M.; Podlasek, C. A.; Serianni, A. S. *J. Am. Chem. Soc.* **1993**, *115*, 10863−70.
(38) Wu, J.; Bondo, P. B.; Vuorinen, T.; Serianni, A. S. *J. Am. Chem. Soc.* **1992**, *114*, 3499−3505.
(39) Brown, J. W.; Wladkowski, B. D. *J. Am. Chem. Soc.* **1996**, *118*, 1190−3.
(40) Ma, B.; Schaefer, H. F. III.; Allinger, N. L. *J. Am. Chem. Soc.* **1998**, *120*, 3411−22.
(41) van Eijck, B. P.; Hooft, R. W. W.; Kroon, J. *J. Phys. Chem.* **1993**, *97*, 12093−9.
(42) Molteni, C.; Parrinello, M. *J. Am. Chem. Soc.* **1998**, *120*, 2168−71.
(43) Simmerling, C.; Fox, T.; Kollman, P. A. *J. Am. Chem. Soc.* **1998**, *120*, 5771−82.
(44) Brown, H. C.; McDonald, G. J. *J. Am. Chem. Soc.* **1966**, *88*, 2514−9.
(45) Brown, H. C.; Azzaro, M. E.; Koelling, J. G.; McDonald, G. J. *J. Am. Chem. Soc.* **1966**, *88*, 2520−5.
(46) Carr, C. A.; Ellison, S. L. R.; Robinson, M. J. T. *Tetrahedron Lett.* **1989**, *30*, 4585−88.
(47) Forsyth, D. A.; Prapansiri, V. *Tetrahedron Lett.* **1988**, *29*, 3551−4.
(48) Carr, C. A.; Robinson, M. J. T.; Young, D. J. *Tetrahedron Lett.* **1989**, *30*, 4593−6.
(49) Carr, C. A.; Robinson, M. J. T.; Webster, A. *Tetrahedron Lett.* **1989**, *30*, 4589−92.
(50) Anet, F. A. L.; Basus, V. J.; Hewett, A. P. W.; Saunders, M. *J. Am. Chem. Soc.* **1980**, *102*, 3945−6.
(51) Williams, I. H. *J. Chem. Soc., Chem. Commun.* **1986**, 627−8.

Materials and Methods

Materials. [1-^{2}H]Glucose was purchased from Sigma Chemical Company (St. Louis, MO). [2-^{2}H]-, [3-^{2}H]-, [4-^{2}H]-, [5-^{2}H]-, and [6,6′-$^2H_2$]glucose were obtained from Omicron Biochemicals (South Bend, IN). Sugars were used without further purification. Methanol was from Fisher Scientific (Pittsburgh, PA) and 5 mm NMR tubes and coaxial inserts were from Wilmad Glass (Buena, NJ). Spectra were collected on a 300 MHz Bruker instrument and quatronuclear probe.

Peak Assignments. The ^{13}C6 signals were assigned using their longer transverse relaxation time. All other signals were unequivocally assigned on the basis of ^{1}H−^{13}C heteronuclear spin correlation spectroscopy and 2D INADEQUATE spectroscopy. ^{13}C assignments were further verified with 1D ^{1}H-decoupled ^{13}C spectra of deuterated glucose.

Equilibrium NMR Spectroscopy. Individual peaks were better resolved in 1D ^{13}C as compared to 1D ^{1}H spectra, and while 2D ^{1}H-COSY was capable of resolving the spectrum, we determined that integrating in two dimensions could add unwanted complications. Further, as we desired to acquire the isotope effect data in aqueous solution, the utilization of 1D ^{1}H NMR was ruled out because the H_2O peak (4.882 ppm) grossly interferes with the α-^{1}H1 and β-^{1}H1 peaks (5.212 and 4.622 ppm, respectively) and because suppression of the water signal could alter the observed integration ratio. Therefore, the data reported here were acquired using inverse-gated ^{1}H-decoupled ^{13}C NMR with an interpulse delay of 8 times the longest carbon T_1. All samples were permitted to equilibrate to 25 °C *in the instrument* prior to data acquisition. The solvent for sugars was H_2O:methanol 9:1, and spectra were collected in 5 mm tubes with D_2O included within a coaxial insert.

Spectral Analysis. The anomeric equilibrium constant, $K_{\beta/\alpha}$, was calculated for unlabeled glucose by dividing the integral over β-^{13}C1 by that over α-^{13}C1 and also by dividing the integral for β-^{13}C(5,3,2) by that for α-^{13}C(5,3,2). The $K_{\beta/\alpha}$ values for deuterated glucose species were calculated by taking the appropriate ratios of peaks which contained no carbon splitting due to deuterium; for example, with [2-^{2}H]-glucose the ^{13}C(5,3,2) signals were not used. Spectra were integrated over a 1 ppm range centered on β- or α-^{13}C1 and/or over a 2.6 ppm range beginning 0.5 ppm downfield of the most shifted peak of the β- or α-^{13}C(5,3,2) clusters. Isotope effects and standard errors were calculated by:

$$^{D}K_{\beta/\alpha} = {}^{1}K_{\beta/\alpha}/{}^{2}K_{\beta/\alpha}$$

$$\sigma_m{}^{D}K = ((\sigma_m{}^{1}K)^2/({}^{2}K)^2 + ({}^{1}K)^2(\sigma_m{}^{2}K)^2/({}^{2}K)^4)^{1/2}$$

where $^1K_{\beta/\alpha}$ and $^2K_{\beta/\alpha}$ are mean values from separate spectra and σ_m are the standard deviation of the mean for those measurements. In the case of [4-^{2}H]- and [6,6′-$^2H_2$]glucose, where two values of $^DK_{\beta/\alpha}$ were obtained, these were further averaged and the variance propagated accordingly to yield the final values.

Semiempirical and ab Initio Calculations. (A) Glucose. Theoretically, there can exist 12 rotamers of $^4C_1$ glucose including two anomers, three rotamers of the extracyclic hydroxymethyl, and two orientations for intramolecular hydrogen bonds between the hydroxyl groups (Figure 1). It has been shown that the barriers to reorganization are large enough to distinguish these ground states in the gas phase and probably in the solution phase, although intramolecular hydrogen bonds are not likely to be as important as glucose−water interactions. Geometry optimizations and frequency calculations were performed for each rotamer using the Gaussian 94 software package.[52]

Geometry results and force constants in Cartesian coordinates were used as input for the program QUIVER,[53] which calculates "fractionation factors" in isotopic exchanges for each species. QUIVER was modified to permit specification of frequency correction factors (PM3, 0.9761, RHF/3-21G, 0.9085, and RHF/6-31G(d,p), 0.8992;[54] DFT, 0.9561[55]). Mole fractions for each species were calculated from the Boltzmann distribution using final energies from the Gaussian 94 geometry jobs. Alternatively, extracyclic hydroxymethyl rotamer mole fractions were taken as in Nishida et al.,[23] and only the relative

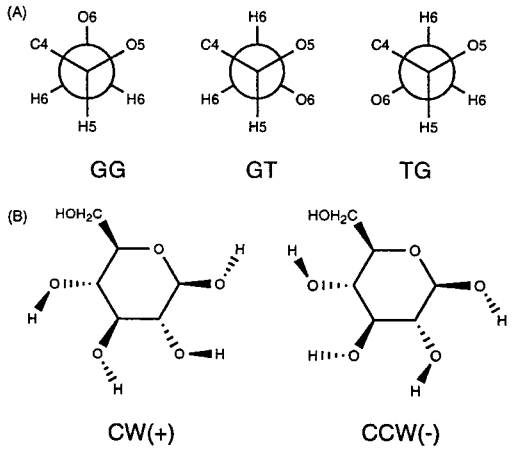

Figure 1. Rotamers of D-glucose in the $^4C_1$ chair. Top row: three low-energy staggered positions of the extracyclic hydroxymethyl group. Bottom row: two orientations of gas-phase intramolecular hydrogen bonds.

abundances of CW(+) and CCW(−) subsets were calculated from Boltzmann distribution as above. These fractionation factors were combined as shown in eq 1,

$$^{D}K = \sum_{i=1}^{6} \varphi^{\chi_{\alpha i}}_{\alpha i}\left(\varphi^{\chi_{\beta i}}_{\beta i}\right)^{-1} \quad (1)$$

where φ_i are the fractionation factors and χ_i are the mole fractions for rotamer *i*. This procedure was carried out using combinations of the PM3, Hartree−Fock, and B3PW91 methods, the 3-21G and 6-31G** basis sets, and the Onsager dipole solvation model ($\epsilon = 78.5$). Energies in kcal/mol due to electron delocalization were calculated by the NBO extension[56−59] of Gaussian 94.

(B) 2-Propanol. Using Gaussian 98,[60] a gas-phase model of 2-propanol was minimized at the RHF/3-21G level of theory with respect to all parameters except the torsional angle, θ, given by $H_C-C_C-O-H_O$ (see Figure 2), which was held fixed at various positions. Force constants in Cartesian coordinates were calculated for each structure and transformed *via* QUIVER into conformational equilibrium isotope effects. Energies due to hyperconjugative electron delocalization and the populations of bonding and antibonding orbitals were calculated by NBO in Gaussian 98.

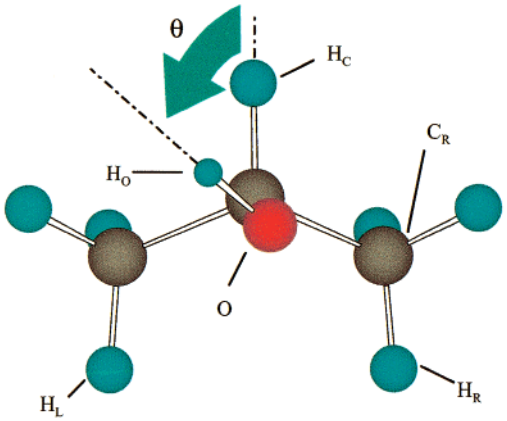

Figure 2. 2-Propanol and $H_C-C_C-O-H_O$ dihedral (θ).

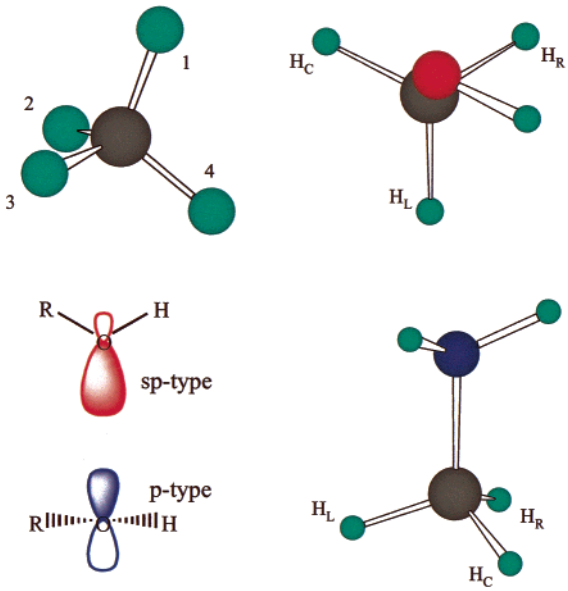

Figure 3. Methane, methanol, methylamine and the p-type and sp-type orbitals for ROH groups (clockwise from upper left).

(C) Methane, Methanol, and Methylamine. Various H−C−H, H−C−O, and H−C−N angles were held fixed, and isotope effects and NBO parameters were calculated as described above for 2-propanol. Atoms are defined as in Figure 3.

(D) Cyclohexane. Calculations were also made on equitorial vs. axial CH bonds in cyclohexane.

Results

Glucose ^{13}C NMR. Sample NMR spectra are shown in Figure 4. Panel A shows a typical ^{1}H spectrum of α/β-equilibrated glucose in D_2O. The anomeric signals flank the residual water peak, and the remainder of the spectrum is sufficiently complicated to rule out the integration of separate peaks. Panels B and C represent ^{13}C spectra of [U-^{1}H]- and [3-^{2}H]glucose, respectively. Carbon signals at 96.3, 92.5, 76.25, 76.25, 74.6, 73.3, 71.9, and 71.8 ppm arise from C1β, C1α, C5β and C3β, C2β, C3α, C5α, and C2α, respectively. This distribution made it possible to integrate the C(5,3,2)β peaks in comparison with the C(3,5,2)α peaks and also the C1β and C1α peaks. Whereas with ^{1}H observation it would have been impossible to acquire the equilibrium constant for [1-^{2}H]glucose, ^{13}C NMR spectroscopy permitted the acquisition of the complete set.

(52) Frisch, M. J.; Trucks, G. W.; Schlegel, H. B.; Gill, P. M. W.; Johnson, B. G.; Robb, M. A.; Cheeseman, J. R.; Keith, T.; Petersson, G. A.; Montgomery, J. A.; Raghavachari, K.; Al-Laham, M. A.; Zakrezewski, V. G.; Ortiz, J. V.; Foresman, J. B.; Cioslowki, J.; Stefanov, B. B.; Nanayakkara, A.; Challacombe, M.; Peng, C. Y.; Ayala, P. Y.; Chen, W.; Wong, M. W.; Andres, J. L.; Replogle, E. S.; Gomperts, R.; Martin, R. L.; Fox, D. J.; Binkley, J. S.; Defrees, D. J.; Baker, J.; Stewart, J. P.; Head-Gordon, M.; Gonzalez, C.; Pople, J. A. *Gaussian 94, Revisions C.2, D.4*; Gaussian, Inc.: Pittsburgh, PA, 1995.

(53) Saunders, M.; Laidig, K. E.; Wolfsberg, M. *J. Am. Chem. Soc.* **1989**, *111*, 8989−94.

(54) Scott, A. P.; Radom, L. *J. Phys. Chem.* **1996**, *100*, 16502−13.

(55) Wong, M. W. *Chem. Phys. Lett.* **1996**, *256*, 391−9.

(56) Glendening, E. D.; Reed, A. E.; Carpenter, J. E.; Weinhold, F. *NBO, Version 3.0*; Theoretical Chemistry Institute and Department of Chemistry, University of Wisconsin: Madison, WI, 1994.

(57) Foster, J. P.; Weinhold, F. *J. Am. Chem. Soc.* **1980**, *102*, 7211−8.

(58) Reed, A. E.; von Rague Schleyer, P. *J. Am. Chem. Soc.* **1987**, *109*, 7362−73.

(59) Reed, A. E.; Curtiss, L. A.; Weinhold, F. *Chem. Rev.* **1988**, *88*, 899−926.

(60) Frisch, M. J.; Trucks, G. W.; Schlegel, H. B.; Scuseria, G. E.; Robb, M. A.; Cheeseman, J. R.; Zakrzewski, V. G.; Montgomery, J. A.; Stratmann, R. E.; Burant, J. C.; Dapprich, S.; Millam, J. M.; Daniels, A. D.; Kudin, K. N.; Strain, M. C.; Farkas, O.; Tomasi, J.; Barone, V.; Cossi, M.; Cammi, R.; Mennucci, B.; Pomelli, C.; Adamo, C.; Clifford, S.; Ochterski, J.; Petersson, G. A.; Ayala, P. Y.; Cui, Q.; Morokuma, K.; Malick, D. K.; Rabuck, A. D.; Raghavachari, K.; Foresman, J. B.; Cioslowski, J.; Ortiz, J. V.; Stefanov, B. B.; Liu, G.; Liashenko, A.; Piskorz, P.; Komaromi, I.; Gomperts, R.; Martin, R. L.; Fox, D. J.; Keith, T.; Al-Laham, M. A.; Peng, C. Y.; Nanayakkara, A.; Gonzalez, C.; Challacombe, M.; Gill, P. M. W.; Johnson, B. G.; Chen, W.; Wong, M. W.; Andres, J. L.; Head-Gordon, M.; Replogle, E. S.; Pople, J. A. *Gaussian 98, Revision A.6*; Gaussian, Inc.: Pittsburgh, PA, 1998.

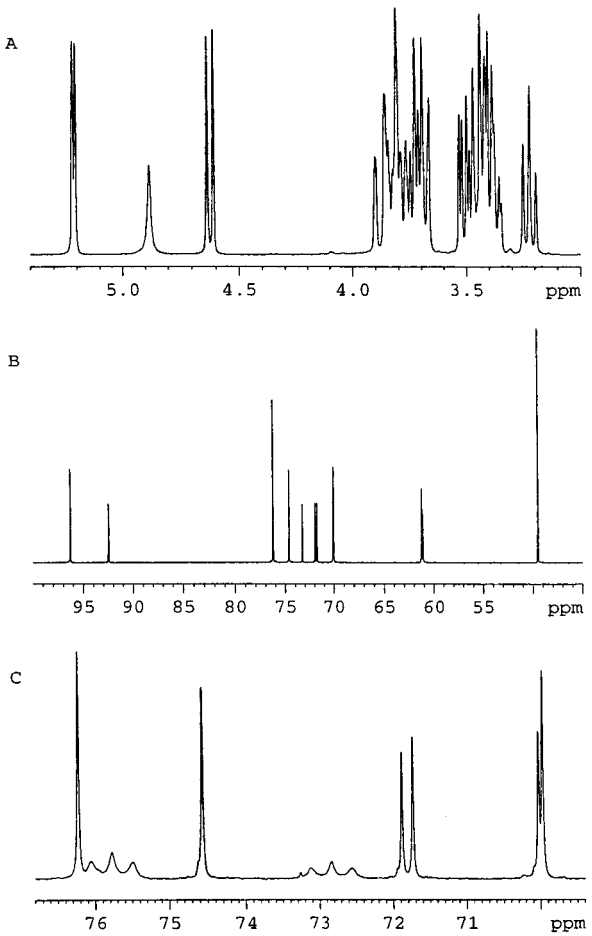

Figure 4. NMR spectra of D-glucose at equilibrium: (A) ^{1}H NMR of glucose in D_2O, 10% CD_3OD; (B and C) ^{1}H-uncoupled ^{13}C NMR of glucose and [3-^{2}H]-glucose, respectively, in H_2O, 10% CH_3OH.

Table 1. Equilibrium Constant, $K_{\beta/\alpha}$, for Aqueous Glucose and Isotope Effects Measured by ^{13}C NMR[a]

label	equilibrium position,[b] $K_{\beta/\alpha}$ $(\beta/\alpha)_1$	$(\beta/\alpha)_{2,3,5}$	n	isotope effect, $^DK_{\beta/\alpha}$
[U-^{1}H]	1.6104 ± 0.0047	1.5721 ± 0.0027	(15)	-
[1-^{2}H]		1.5076 ± 0.0059	(7)	1.043 ± 0.004
[2-^{2}H]	1.5681 ± 0.0068		(8)	1.027 ± 0.005
[3-^{2}H]	1.5676 ± 0.0046		(12)	1.027 ± 0.004
[4-^{2}H]	1.6196 ± 0.0054	1.5612 ± 0.0049	(3)	1.001 ± 0.003
[5-^{2}H]	1.5538 ± 0.0039		(3)	1.036 ± 0.004
[6,6-$^2H_2$]	1.6043 ± 0.0097	1.5838 ± 0.0068	(8)	0.998 ± 0.004

[a] In H_2O, 10% MeOH. [b] From the ratio of integration of the C1(β/α) peaks or the C2,3,5(β/α) peaks.

The isotope effects measured in this way are listed in Table 1. The equilibrium constant derived from the integrations $(\beta/\alpha)_1$ and $(\beta/\alpha)_{5,3,2}$ are shown for each molecule. Significant normal isotope effects can be seen at H1, H2, H3, and H5. Effects of unity are seen at H4 and H6 (performed with [6,6′-$^2H_2$]glucose). Whereas $^DK_{\beta/\alpha}$ differed slightly between peak sets in the case of [U-^{1}H]-, [4-^{2}H]-, and [6,6′-$^2H_2$]glucose, this was assumed not to vary between the molecules.[61] The CH bonds which appear to differ vibrationally between α- and β-glucose correspond precisely to those nuclei which have different chemical shifts by ^{1}H and ^{13}C NMR. In other words, C1, C2, C3, and C5 are downfield in β-glucose from their α counterparts and are therefore less shielded in the β-sugar. The converse is true in the ^{1}H spectrum. These relations are summarized in Table 2. Isotope effects on ^{13}C chemical shift were also observed as shown in Figure 4c.

(61) As these signals arise from different sugars trace-labeled at either C1, C2, C3, or C5, this difference could arise from a carbon anomeric isotope effect. However, carbon effects never exceed 1%. Therefore, the different choice of integration ranges is probably responsible.

Table 2. Chemical Shift[a] and Observed Isotope Effect in Glucose

		^{1}H NMR (ppm)		^{13}C NMR (ppm)	
	CEIE[b]	α	β	α	β
CH1	1.043	5.09	4.51	92.9	96.7
CH2	1.027	3.41	3.13	72.5	75.1
CH3	1.027	3.61	3.37	73.8	76.7
CH4	1.001	3.29	3.30	70.6	70.6
CH5	1.036	3.72	3.35	72.3	76.8
pro*R*-CH6		3.72	3.75		
	0.998			61.6	61.7
pro*S*-CH6		3.63	3.60		

[a] Reference 28. [b] From Table 1.

Table 3. Calculated Anomeric Equilibrium Isotope Effects for Glucose

		gas phase				Onsager, $e = 78.8$	
		Hartree−Fock				Hartree−Fock	
label	expt	PM3	3-21G	6-31G**	B3PW91[a]	3-21G	6-31G**
[1-^{2}H]	1.043	1.047	1.021	1.057	1.079	1.024	1.057
[2-^{2}H]	1.027	1.035	1.019	1.041	1.058	1.027	1.046
[3-^{2}H]	1.027	1.001	1.045	1.013	1.012	1.041	1.011
[4-^{2}H]	1.001	0.989	0.977	0.986	0.989	0.985	0.986
[5-^{2}H]	1.036	1.010	1.032	1.040	1.035	1.030	1.038
[6(*S*)-^{2}H]		1.013	1.014	1.014	1.013	1.007	1.011
[6(*R*)-^{2}H]		0.995	0.985	0.984	0.983	0.993	0.986
[6,6′-$^2H_2$]	0.998	1.008	0.998	0.998	0.996	0.999	0.997
[5-^{18}O]		0.992	1.003	1.000	1.000	1.002	1.000
Hybrid-Calculated Isotope Effects Incorporating Experimental Mole Fractions[b]							
[1-^{2}H]	1.043	1.045	1.019	1.056	1.077	1.019	1.057
[2-^{2}H]	1.027	1.027	1.030	1.043	1.057	1.030	1.046
[3-^{2}H]	1.027	1.001	1.036	1.011	1.012	1.039	1.028
[4-^{2}H]	1.001	0.987	0.994	0.998	0.994	0.999	0.987
[5-^{2}H]	1.036	1.010	1.024	1.036	1.036	1.026	1.035
[6(*S*)-^{2}H]		0.978	1.000	1.007	1.012	1.003	1.036
[6(*R*)-^{2}H]		1.026	0.999	1.001	0.998	0.999	0.997
[6,6′-$^2H_2$]	0.998	1.004	0.999	1.008	1.010	1.002	1.030
[5-^{18}O]		0.993	1.002	0.999	1.000	1.001	0.999

[a] 6-31G**, no solvation. [b] Reference 23.

Calculations on Glucose. Comparison by Level of Theory and Basis Set. The calculations performed at RHF/6-31G** (Table 3a) best matched the ^{13}C NMR data. These show the largest effect at H1 followed by H2 and H5, with no effect at H6. While the model yields different isotope effects for H2 and H3 (1.046 and 1.011, respectively), the values are equidistant from the experimental values of 1.027 for these atoms. Including a solvent dielectric as in the Onsager dipole model contributed little to the RHF/3-21G or RHF/6-31G** models. Isotope effects at H1 and H2 were greatly exaggerated in the density functional model (B3PW91/6-31G**), and the PM3 model performed well except at protons H3 and H5. All models compute an inverse isotope effect at H4, a different isotope effect between the two extracyclic methylene protons, and, except for PM3, no significant ^{18}O isotope effect.

Hybrid Calculations: Experimental Mole Fractions. Where the fractionation factors were combined according to the mole fractions experimentally determined by Nishida et al.,[23] the results for each model were generally improved, particularly for H3, H4, and H5 (Table 3b). The exceptions here are the Onsager RHF/6-31G** calculations for the H6 protons, which change from unity to one or three percent.

Correlations with Isotope Effect in 6-31G Calculations.** The RHF/6-31G**-Onsager dipole calculations were used to

Table 4. Geometry and Electronic Changes in Representative Models of Glucose Anomers[a]

		bond length (Å)		bond order change[b]	hyperconjugation[c] (kcal/mol)					orbital changes[d]			
					α		β			α	carbon	β	carbon
CH	CEIE	α	β	Δσ−σ*	σ→	→σ*	σ→	→σ*	ΔΣ(β−α)	hybrid.	cont. (%)	hybrid.	cont. (%)
1	1.054	1.083	1.091	−0.00802	12.08	2.44	9.90	9.77[e]	5.15	$sp^{2.70}$	60.53	$sp^{2.74}$	59.37
2	1.048	1.084	1.088	−0.00247	15.54	2.97	13.69	10.00[f]	5.18	$sp^{3.12}$	61.53	$sp^{3.04}$	61.20
3	1.011	1.089	1.090	−0.00072	12.42	10.27	12.99[g]	10.19	0.49	$sp^{3.11}$	60.78	$sp^{3.16}$	60.63
4	0.996	1.087	1.087	−0.00004	12.22	10.82	12.43	10.75	0.14	$sp^{3.04}$	61.32	$sp^{3.02}$	61.46
5	1.036	1.086	1.090	−0.00215	11.61	9.23	11.70	9.65[h]	0.51	$sp^{3.00}$	61.28	$sp^{3.07}$	60.71
6-*pro*S	1.000	1.088	1.088	−0.00027	6.39	10.31	6.47	10.49	0.26	$sp^{2.97}$	59.75	$sp^{2.96}$	59.80
6-*pro*R	1.000	1.081	1.081	−0.00027	11.07	2.16	10.92	2.18	-0.13	$sp^{2.94}$	61.36	$sp^{2.94}$	61.34

[a] RHF/6-31G** Onsager dipole models α-gg(−) and β-gg(−) only. [b] Calculated by subtracting the number of electrons occupying the σ* orbital from the number occupying the σ orbital and listed as the change between α- and β-glucose. [c] Sum of second-order perturbation contributions calculated by NBO analysis. Cutoff = 0.5 kcal/mol. [d] Hybridization of the carbon atom and contribution of the carbon atom to the bond in percent. [e−h] Lp1 is the sp-type lone pair, and Lp2 is the p-type lone pair: [e]Lp2(O5); [f]Lp2,1(O2); [g]C2, C2−H2, and C2−O2 are better acceptors in β; [h]while Lp2(O5) declines in β, Lp1(O5) increases by 1 kcal/mol.

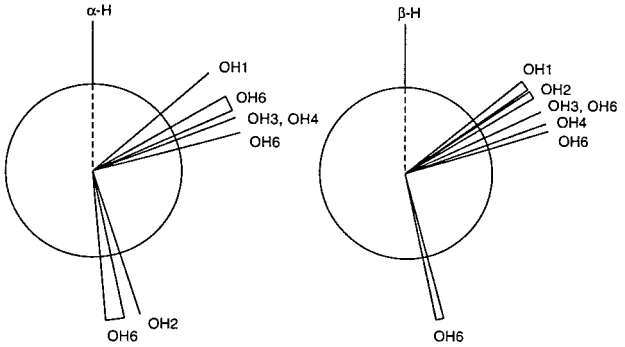

Figure 5. Dihedral angle summary for hydroxyl groups in (A) α-glucose and (B) β-glucose at RHF/6-31G** (Onsager dielectric $\epsilon = 78.8$). Backbone protons are all represented in the north position here for comparison. The large circles, the vertices, and the line ends represent the backbone carbons, the hydroxyl oxygens, and the hydroxyl protons, respectively. The ends of identically labeled lines are connected for clarity.

explore the anomeric differences since these proved superior in predicting the atoms of largest and smallest isotope effect. The calculations predict three major contributors (gg(−), gt(−), and tg(−)) to the α-glucose population mixture and, therefore, to its fractionation factor and two major contributors (gg(−) and gt(−)) for β-glucose. We only present the data from these major species.

We observe in these gas-phase calculations that only the 2-hydroxyl changes significantly in dihedral angle between α- and β-glucose (Figure 5). In α-glucose, the dihedral angle H2−C2−O2−OH2 has a value of approximately 160° for all three models, and in β-glucose, these have changed to about 60° for both models. The respective angles permit intramolecular hydrogen bonding to exist in the gas phase between the 2-hydroxyl and the 1-hydroxyl. The gg(−) models were taken as representative for both α- and β-glucose and were therefore examined by natural bond orbital analysis (Table 4). For all protons in these models, CEIE correlates with bond length and bond order changes. Bond lengthening and bond order decreases in β-glucose yield normal equilibrium isotope effects. Further, a decrease in the orbital coefficient of the sp^3 orbital donated by the carbon atom indicates bond polarization toward the proton, and here this parameter is seen to correlate notably well with CEIE and with the observed anomeric differences in ^1H and ^{13}C chemical shift. Except for H1 and H2, carbon hybridization also correlates with isotope effect.

In summing over second-order perturbation energies above the cutoff of 0.5 kcal/mol,[62] it was observed that both H1 and H2 benefit from a significant increase in electron delocalization into their respective σ* orbitals. The source of this electron density for H1 is the p-type lone-pair of the ring oxygen, O5, and for H2 it is mostly the p-type lone pair with some contribution from the sp-type lone pair of O2. The energies derived from these delocalizations are a full order of magnitude greater than the corresponding differences for the H3 and H5 protons in α- and β-glucose. In the case of the latter protons, the majority of delocalization energy derives from increased overlap of the bonding σ orbital of C3−H3 with the antiperiplanar C2−H2 and the C2−O2 antibonding σ* orbitals and from a slightly increased donation by the p-type O5 ring oxygen lone pair into the σ* orbital of C5−H5. The C4−H4 and C6−H6 bonds show no difference in electron delocalization.

Whereas hyperconjugation is dominant for H1 and H2, steric factors correlate with the isotope effects at H3 and H5. In α-glucose, the 1-hydroxyl group is axial and might be expected to interact sterically with the syn-diaxial H3 and H5 protons. Examination of the same gg(−) models demonstrates that the H3−O1 distance of 2.64 Å and the H5−O1 distance of 2.63 Å are both inside the minimum radius expected for van der Waals repulsion (2.72 Å). This strain is fully relieved in β-glucose where the H3−H1 distance of 2.44 Å and the H5−H1 distance of 2.54 Å are both outside the van der Waals radius expected for two protons (2.40 Å). Comparison of the two models in Figure 6 shows that in α-glucose the H3 and H5 protons are strained away from the anomeric center. This strain is nonetheless insufficient to fully relieve the van der Waals radius impingement. The same protons in β-glucose appear relaxed and truly syn-diaxial with H1. These observations are mirrored precisely in the RHF/3-21G calculations, in which this steric interaction seems to be the dominant effect.

Conformational Equilibrium Isotope Effects in 2-Propanol. 2-Propanol was selected as a small molecular model for conformational isotope effects pertinent to glucose. We found that varying the central $H_C-C_C-O-H_O$ dihedral angle in 2-propanol gives significant changes in the fractionation factor for all protons and for H−C distances and C−C distances (Figure 7). Reported here are properties for the central proton H_C and for the two antiperiplanar methyl protons H_R and H_L. For every dihedral angle calculated, H_R and H_L minimized precisely antiperiplanar to H_C. Taking the dihedral angle of 59.9° as the reference state (panel A), H_C has a normal isotope effect of 1.005 at 0° and an inverse isotope effect of 0.950 at 180°. The other two protons, H_R and H_L, vary with each other and inversely with respect to the central proton. Each experiences a

(62) Summing with such a low cutoff energy may lead to errors since some values will be within the errors expected for these calculations. However, the use of higher cutoff values led to similar results (compare Table S1, Supporting Information).

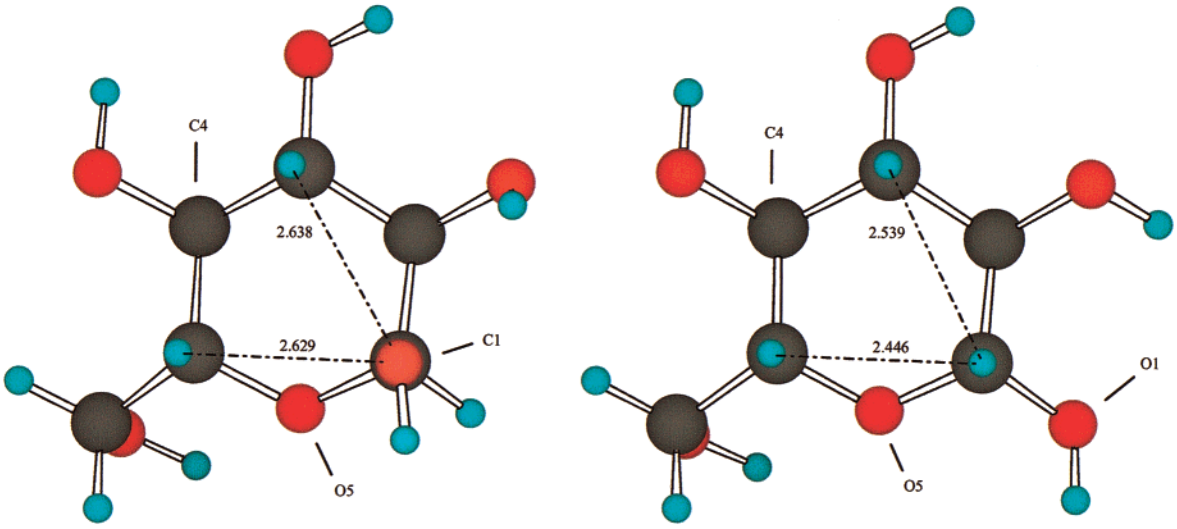

Figure 6. Syn-diaxial repulsion and relief in glucose. The protons H3 and H5 appear syn-diaxial with the anomeric substituent in the β-gg(−) rotamer (right) and off-center in the α-gg(−) rotamer (left). These models at RHF/6-31G** Onsager resembled those at RHF/3-21G Onsager.

slight inverse effect of 0.997 at 0° and a much larger normal effect of 1.025 at 180°. A normal isotope effect indicates a vibrationally looser environment for the proton than it experiences where the dihedral angle is minimized to 59.9°. As expected, these isotope effects correlate well with C−H bond length changes as a function of dihedral angle (panel B); the central bond decreases from 1.0850 to 1.0785 Å and the H_R and H_L lengths increase from 1.0825 to 1.0865 Å at 0° and 180°, respectively. The C_C-C_R and C_C-C_L distances (panel C) also varied with central dihedral angle, from 1.528 to 1.532 Å at 0° and 180°, respectively. The bond lengths for H_R and H_L and for C_C-C_R and C_C-C_R vary quite asymmetrically but superimpose at 0° and 180° as expected. Finally, we observe a significant change in the H_C-C_C-O angle with dihedral. Figure 7D shows this correlation overlaid with the angles and dihedrals for the protons in glucose from the two most abundant rotamers (α-gg(−) and β-gg(−)). As the dihedral is changed from 0° to 180°, H_C-C_C-O becomes more acute from 110.4° to 104.5°.

A concern in this type of study is that equilibrium isotope effects may be improperly calculated if one part of the molecule is held at a nonequilibrium position. In the present case, visualization of the modes consisting primarily of H_C-C stretch and $H_C-C_C-O-H_O$ angle libration demonstrated complete decoupling with respective frequencies of 2800 and 280 cm^{-1}. This evidence, coupled with the smooth variation of ^2H isotope effects and bond lengths as dihedral is varied from 0° through a global energy minimum at 60° and finally to 180°, is sufficient to disqualify this concern.

Electron delocalization energies and population transfers were observed to vary with the dihedral angle (Figure 8). Panel A shows energy stabilization due to n → σ* hyperconjugation by the oxygen lone pairs into the antibonding orbital of H_C-C_C. The contribution due to the p-type (○) lone pair is greatest at 90° and that due to the sp-type lone pair (△) is greatest at 0° and 180° with a nadir at 90°; these are precisely as expected due to geometric overlap of the respective lone pairs with the H_C-C_C bond. The total population of the antibonding σ* orbital (panel B) directly follows the total energy (●) shown in panel A and takes its dominant contribution from the p-type lone pair. The population of the σ bonding orbital of the H_C-C_C bond also demonstrates angular dependence, with its maximum loss at 180°, corresponding to maximum overlap with the σ* orbital of an antiperiplanar $O-H_O$ bond. As the angle is changed from 180° to 90°, it is clear that the isotope effect can be explained by increasing hyperconjugative overlap. But in the region 90° to 0°, this overlap decreases but the isotope effects become even larger. Remarkably, this is due to relief in this region of steric impingement of the C_C-H_C bond by the bulky oxygen sp-type and p-type lone pairs. The back lobe of the sp-type lone pair which interacts with the CH bond at 0° is much smaller than its main lobe or either p-type lobe visualized by NBO.

Calculations on Other Model Compounds. A brief analysis of the data in Table 5 will assist in interpreting the calculations on glucose below. Altering the normally 109.4° tetrahedral angle of methane to 114° affects bond polarity, carbon hybridization, and bond length. The two protons which were moved apart, H1 and H4 in our model, are bonded to carbon hybrid orbitals with less p-character than the remaining protons. The greater s-character correlates with the shorter bonds, and the C−H1 and C−H4 bonds are also more polarized toward carbon. A conformational equilibrium isotope effect calculation here yields unity for exchange of H1 or H4 with either of the other protons. The unperturbed symmetrical protons H_L and H_R of methanol benefit from significant hyperconjugative charge transfer from the p-type oxygen lone pair, paralleling the behavior of C−C bonds in 2-propanol above, and consequently have longer CH bonds and a significant CEIE of exchange (1.046) with H_C (see Figure 3 for atom lettering). These protons make a much larger angle with the oxygen than does H_C, a change that increases the back-lobe overlap, and their bonds are more polarized toward the carbon atom. The carbon hybrids paired with H_L and H_R have less p-character as well. Decreasing this back-lobe overlap by fixing H_R-C-O at 108° affects the moved atom only with a 2% inverse CEIE, decreased hyperconjugation by 2 kcal/mol and increased carbon hybrid p-character. Increasing the H_R-C-H_C angle by 5° to 112° alters the carbon hybrids toward all three protons but effects barely a 1% inverse CEIE on H5. This calculation was made holding $H_C-C-O-OH$ and $H_L-C-O-OH$ fixed in order to isolate H5 movement. Finally, the nitrogen lone pair in methylamine delocalizes into the σ* orbital of $C-H_C$ with an associated energy of 11 kcal/mol, a longer, more carbon-polarized CH bond, an increased H_C-C-N angle, and a CEIE of 1.041 for exchange of either H_L or H_R in place of H_C.

In cyclohexane at RHF/3-21G, an axial CH bond benefits from transfer (4 times 3.03 kcal/mol) donative to and receptive from each of its two antiperiplanar partners, whereas an equatorial CH bond benefits from a donative interaction (3.56 kcal/mol) and a receptive interaction (2.08 kcal/mol) with each

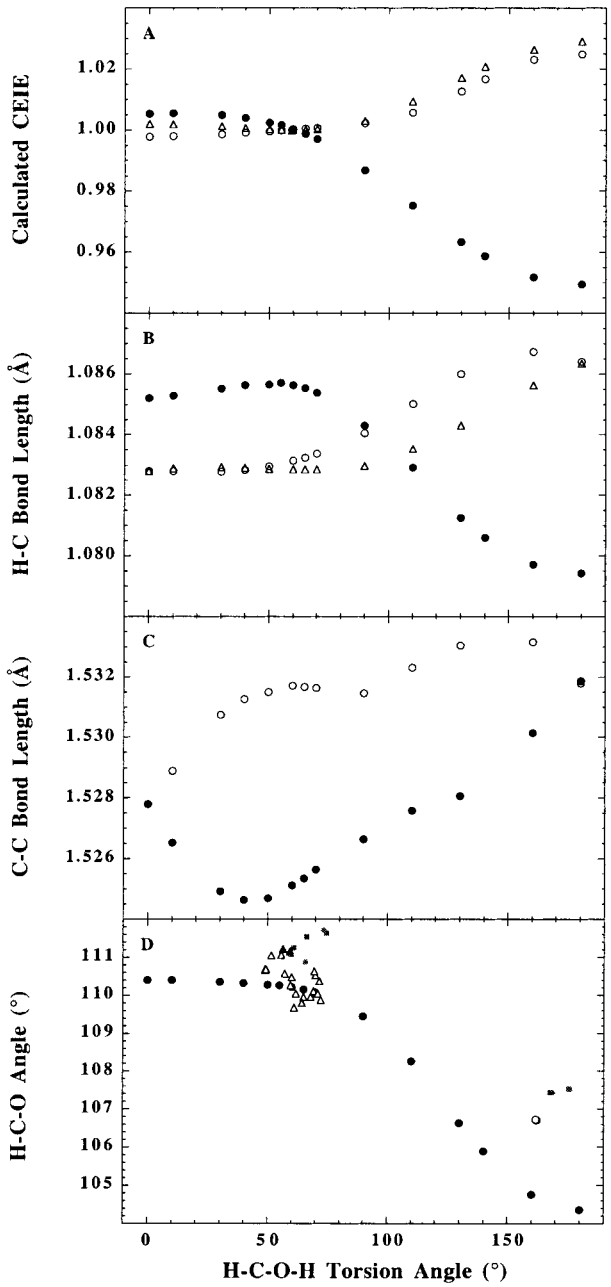

Figure 7. C−O dihedral angle effects in gas-phase 2-propanol at RHF/3-21G: (A) CEIE for H_C (●), H_R (○), and H_L (△) from reference point of 60°; (B) bond lengths for protons in (A); (C) C_C-C_L (○) and C_C-C_R (●) bond length versus dihedral angle; (D) H_C-C_C-O angle (●) also varies with dihedral angle; overlaid are α-H2 (○), *β*-H2 (○), α-H6 (▲), *β*-H6 (■), and other backbone protons (●) from the glucose models.

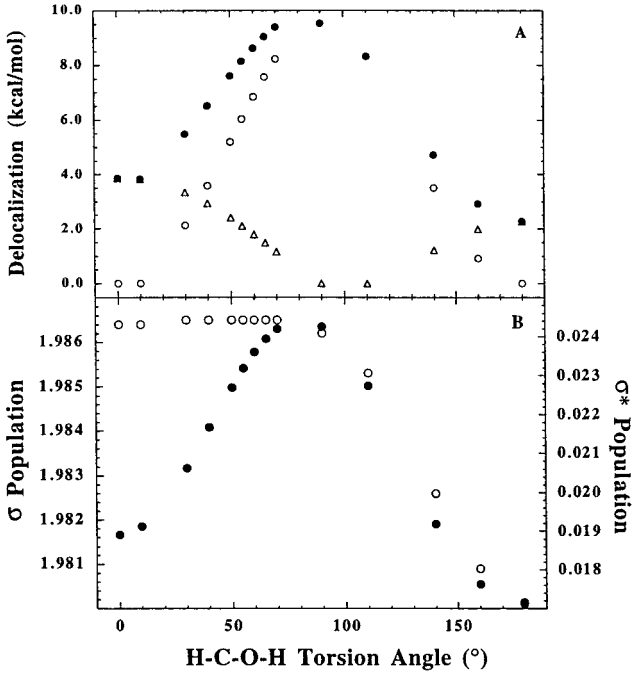

Figure 8. Hyperconjugative effects in the H_C-C_C bond vary with C_C-O dihedral angle in 2-propanol: (A) delocalization energy in kcal/mol due to overlap of the p-type oxygen lone pair (○), the sp-type oxygen lone pair (△), and the sum of these (●) with the antibonding *σ** orbital; (B) variance of electron population in *σ* orbital (○) and *σ** orbital (●) with dihedral angle.

of two antiperiplanar CC bonds. Therefore, in cyclohexane an axial CH bond is loosened by a net 1 kcal/mol over the equatorial bond, consistent with the conclusions drawn previously in the same system.[6,51] The same NBO analysis shows differences in carbon hybridization for axial ($sp^{3.20}$) and equatorial ($sp^{3.04}$) bonds with corresponding bond length differences.

Several associations can be made from these models. First, unperturbed hyperconjugation causes a much larger isotope effect than the structural perturbations illustrated here. Second, hyperconjugative delocalization yields the dominant effects on electronic configuration. In methanol, the larger $H_{L(R)}-C-O$ angles should be accompanied by much less p-character and much shorter and more carbon-polarized bonds. The results demonstrate the opposite trend for these parameters. The pure p-type oxygen lone pair causes $C-H_{L(R)}$ to become more p-like than expected to increase overlap, the hyperconjugative population of *σ** for these CH bonds lengthens them instead, and we see that the CH bonds are less carbon-polarized where there is more delocalization. Comparison with the sp^6-hybridized nitrogen lone pair of methylamine illustrates that target bond rehybridization is acutely sensitive to lone pair composition. In this case, the difference in p-character between methyl protons is double that in methanol, indicating that the diluted p-character of this lone pair is not as effective in offsetting the increased s-character of the hybrid due to linear angle increase.

Discussion

Isotope Effects at H1 and H2. The experimental equilibrium isotope effects with glucose can be explained fully in terms of phenomena observed in gas-phase models. A significant normal isotope effect of 1.043 is observed at H1. Simple axial−equatorial isotope effects are already well documented. Deuterium isotope effect studies in cyclohexane have reported an observed value[63] of 1.060 at −88 °C and a calculated value[51] of 1.039 at the same temperature. These values translate to free energy differences of 91 and 59 J/mol and isotope effects of 1.037 and 1.024 at 25 °C, respectively. All of these values favor deuterium equatorially, similar to the preference in glucose. This is consistent with previous work[25] which concluded from the ∼10 Hz greater coupling constant $^1J_{C1H1}$ of α-glucose in solution that the C1−H1 bond is longer[64] when axial in *β*-glucose than when it is equatorial in α-glucose. However, a closer look at the difference in structure between cyclohexane and glucose rules out these axial−equatorial differences as dominant in the

(63) Ayden, R.; Gunther, H. *Angew. Chem., Int. Ed. Engl.* **1981**, *20*, 985.

(64) Maciel, G. E.; McIver, J. W. J.; Ostlund, N. S.; Pople, J. A. *J. Am. Chem. Soc.* **1970**, *92*, 11−18.

Table 5. Reflection of Distortion in Electronic Parameters of Diastereomeric Protons of Model Compounds[a]

compound	H	H−C−X angle[b]	C hybrid.	CH length (Å)	C cont %	hyperconj. (kcal/mol)[c]	CEIE
CH_4	1,4	114.1	$sp^{2.89}$	1.082	61.09	n/a	1.001[d]
	2,3	108.4	$sp^{3.11}$	1.085	60.98		
MeOH	H_L,H_R	112.2	$sp^{2.83}$	1.088	59.14	8.4+1.8	1.046[d]
	H_C	107.3	$sp^{2.87}$	1.081	60.16	2.3	
MeOH(H_R-C−O→108°)	H_R	108.0	$sp^{2.89}$	1.088	59.12	6.8+1.8	0.981[e]
	H_C	107.8	$sp^{2.79}$	1.081	60.19	2.2	1.001[e]
	H_L	112.7	$sp^{2.76}$	1.087	59.20	8.8+1.4	0.999[e]
MeOH(H_R−C−H_C→112°)	H_R	110.9	$sp^{2.81}$	1.088	59.13	7.5+1.9	0.993[e]
	H_C	106.6	$sp^{2.75}$	1.080	60.24	2.2	0.996[e]
	H_L	111.7	$sp^{2.90}$	1.089	59.08	8.6+1.5	1.000[e]
CH_3NH_2	H_C	114.9	$sp^{2.91}$	1.092	59.48	11.21	1.041[d]
	H_L,H_R	109.3	$sp^{3.02}$	1.085	60.50	1.50	

[a] For models in Figure 3 calculated at RHF/6-31G**. [b] In methane, X = H (the other in pair). For other models, X = O,N. [c] Sums represent p-type plus sp-type. Single values indicate p-type contribution only. [d] Exchange. [e] With respect to the same proton in MeOH.

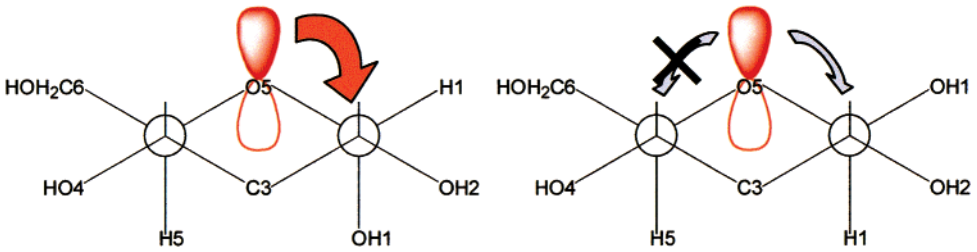

Figure 9. Ring-oxygen lone-pair electron delocalization in glucose anomers. The anomeric effect in α-glucose (left) is the result of $n_p \rightarrow \sigma^*$ hyperconjugation to the axial anomeric hydroxyl. In β-glucose (right) the same hyperconjugative effect loosens the axial C1−H1 bond but gives only a minor contribution to the C5−H5 bond.

latter molecule. The equatorial CH1 in α-glucose would be expected to benefit more from its antiperiplanar relationship with the C2−C3 and O5−C5 bonds than the CH1 in β-glucose, which possesses only an antiperiplanar relationship with CH2. This is confirmed in the α-sugar; the equatorial CH1 is loosened much more by C2−C3 (donative, 3.60 kcal/mol; receptive 2.21) and by O5−C5 (donative, 5.15; receptive, 1.59) than the axial CH1 is loosened by CH2 (donative, 3.22; receptive, 3.89). Thus, a tightening effect at β-H1 is due to a loss of an antiperiplanar bond partner. However, the axial CH1 in β-glucose benefits from interaction with the lone pairs of ring oxygen O5 (receptive from p-type, 8.01; receptive from sp-type, 1.76). There is a greater delocalization of the same lone pair in α-glucose (the anomeric effect), but its target is the axial C1−O1 bond, stabilizing the otherwise much less favorable α-sugar (Figure 9). The isotope effect at H1 is the superposition of two effects, the unfavorable loss of antiperiplanar overlap energy in the β-sugar combined with the favorable increased overlap with the p-type lone pair of O5. The C1−H1 bond in β-glucose experiences a net delocalization of 5.15 kcal/mol, consistent with conclusions drawn previously in the same system.[6,51]

Stereochemically, CH2 shares an antiperiplanar relationship with different partners in α- and β-glucose and consequently experiences different hyperconjugative energies in the two anomers. In α-glucose, CH2 is loosened by C1−O1 (donative, 4.89; receptive, 1.51) whereas in the β-sugar, CH2 is loosened by CH1 (donative, 3.89; receptive, 3.22). These energies predict a slight (0.71 kcal/mol) net effect to loosen the CH1 bond in the β-sugar, but the majority of the isotope effect arises from the difference in orientation of OH2. In the β-sugar, there is significant donation from the lone pairs of O2 (p-type, 6.84; sp-type, 3.16) into σ*-C2−H2. The same bond in the α-sugar interacts only with the O2−OH2 bond (donative, 3.82; receptive, 3.37). Hence another 3 kcal/mol comes from this difference in hydroxyl orientation, leaving the CH2 bond in β-glucose with a net loosening interaction of about 4 kcal/mol.

Our models show the gas-phase preference in α-glucose for a torsional angle of 160° compared to 60° in β-glucose, in agreement with past work.[15] According to our calculations of 2-propanol, a 160° to 60° change would result in a normal isotope effect at H2 of approximately 5%. This is more than sufficient to account for our measured isotope effect of 2.7%, and the discrepancy leaves room both for level-of-theory dependency and for incomplete rotational restriction in solution, which would tend to dilute a larger effect toward unity. These results strongly imply that in solution the 2-hydroxyl of each anomer at least partially prefers a different angle. The correlation of linear angle and torsional angle for H2 protons with those in 2-propanol (Figure 7D) implies further that the same mechanism is at work.

Isotope Effects at H3 and H5. Scaling the 2-propanol calculations to match the CEIE at H2 results in an inverse contribution of approximately 1.3% to the experimental isotope effects at H1 and H3. Each of these isotope effects would then result from a combination of the effect secondary to the 2-hydroxyl torsional change and a larger normal contribution due to some other effect. While both sites experience significant isotope effects, neither C3−O3 nor C5−O5 torsional angles undergo any real change in geometry between the anomeric ensembles, and the anomeric difference in hyperconjugative energies experienced by the respective bonds are an order of magnitude smaller than those for H1 and H2. Although our calculations on geometry perturbations of hyperconjugated protons in methanol showed that a 5° H−C−O angle increase can yield a 2% isotope effect, neither H3 nor H5 in α-glucose appears to move in this most sensitive direction. The H−C−C(O) angles for these protons remain very similar between anomers. Instead we propose that these isotope effects result from hindered angle bending motions by the axial O2 in α-glucose. In this anomer, both protons are within the minimum O−H van der Waals radius of 2.72 Å. In the β-anomer, H1 instead is syn-diaxial with H3 and H5 and all three protons are

outside the H−H van der Waals radius of 2.40 Å. Deuterium atoms favor the more vibrationally restricted conformation,[44,45,65] since deuterium atoms are effectively smaller than protons in CH bonds.[50]

The hyperconjugative advantage in β-glucose comes from increased antiperiplanar overlap in its less-strained structure; the increased planarity of H5−C5−O5 sp-type and H3−C3−C2−H2 in β-glucose is slightly offset by decreased planarity of 1° between each pair and C4−H4. This different combination of effects at H3 and H5 could account for the different isotope effects. The latter hyperconjugative effects would also contribute in the correct direction to the bond polarity changes seen at these protons but are insufficient on their own to be the sole cause of the observed isotope effects. It is also interesting to note that hyperconjugation plays no larger a role at C5 than at C3. It is expected that the p-type lone pair of O5 would have a higher reduction potential since it does not participate in the anomeric effect, and therefore it would tend to delocalize more into the antibonding orbital σ^* of C5−H5. Instead, as mentioned above, the increased hyperconjugation at H5 in the β-anomer is probably mostly geometrically driven.

Isotope Effects at H6. The magnetic nonequivalence of the methylene protons observed by Nishida in glucose mirrors similar results in aqueous and DMSO solutions of nucleosides[66] and clearly implies some restricted motion about the C5−C6 or C6−O6 bonds. That this nonequivalence is mainly preserved between anomers implies that there is no anomeric effect on this rotational restriction. The latter statement is consistent with our findings of no overall anomeric isotope effect at C6. However, the more telling experiment here involves measuring the anomeric isotope effect of the stereospecifically labeled compounds; as Nishida reports, there is some change in chemical shift for each proton between anomers. Whether this would translate into an observable isotope effect outside the error range of our measurements remains a question.

Curiously, the gg(−) models which we have presented in this report demonstrate the opposite difference in chemical shift to that observed by Nishida. Since greater carbon atom p-orbital character corresponds to longer bonds and greater shielding and more H-polarized CH bonds also correspond to greater proton shielding, we would expect the 6-pro*S* proton to shift at a higher field than the 6-pro*R* proton, contrary to Nishida's findings. While these trends are reverse in gt(−) models (for structures see Supplemental Listing 1), this should be insufficient to account for the discrepancy because Nishida finds the gg rotamers to dominate by 10%.

Intramolecular Hydrogen Bonds. At this point we wish to distinguish that intramolecular hydrogen bonds are not a prerequisite to preferred hydroxyl angles in solution. The role of intramolecular hydrogen bonds in aqueous solutions has been debated. Dais and Perlin[67] concluded that the terminal hydroxyls of D-fructose in D_2O are more intramolecularly hydrogen bonded in the α-furanose form than in either the β-furanose or β-pyranose forms, indicating that some conformers show *intra*molecular hydrogen bonding even in aqueous solutions, but Molteni and Parrinello[42] report finding no evidence of intramolecular bonding in their MD study of aqueous glucose. Simmerling et al.[43] observe in their molecular dynamics studies the existence of preferred hydroxyl torsional angles in solution for the α-anomer of glucose. While those authors do not present data for the β-anomer, we would expect similar results here also, possibly including some changes in angle preference. We favor the latter interpretation of those authors' results as indicative merely of angle preferences and make note that neither our data nor our theoretical models comment on the presence of intramolecular hydgrogen bonds in aqueous solution. Even whether they may be more important for one of the anomers cannot be established from the present results.

Solvation. In their simulations, Molteni and Parrinello[42] found there to be a tighter hydration shell around the anomeric hydroxyl for the α-sugar in solution. This shell would necessarily be accompanied by tighter hydrogen bonds. Gawlita et al.[68] have shown in 2-propanol that the α-proton is highly sensitive to hydrogen bond strength, benefiting from an increase in σ^* population when the oxygen atom more strongly shares its proton with another heteroatom. This effect can be balanced to unity by a counteracting H-bond reception. However, as the precise lattice structure of H_2O around either anomer is unknown, it is not possible to tell at this time whether to expect H-bond donative or receptive interactions to be favored by hydration shell tightening.

γ-Substituent Effect. Finally, is it possible that the γ-substituent effect[69−71] may contribute to the isotope effect and chemical shift change at both C3 and C5? Chemical shift studies in substituted cyclohexanes, dioxanes, and steroids have shown that a γ-anti electronegative atom will cause an upfield or more shielded ^{13}C shift[71−74] unless the carbon serves as a bridgehead atom, where the trend is reversed.[71] A γ-gauche electronegative substituent will cause a downfield shift.[72] The axial 1-hydroxyl of α-glucose is gauche to both C3 and C5, while the equatorial hydroxyl is γ-anti in the β-anomer. Since the change from α-glucose to β-glucose is equivalent to a change from γ-gauche to γ-anti, the chemical shift of C3 and C5 would be expected to move upfield. Instead, we observe a downfield shift in β-glucose. Furthermore, ^1H and ^{13}C shifts vary together with increasing electronegativity of the γ-anti atom,[74] whereas in β-glucose C3 and C5 are less shielded while the corresponding protons H3 and H5 are more shielded. Thus, we conclude that the classic γ-substituent effect plays no role in glucose.

Bond Polarizations and Chemical Shifts. Previous studies have demonstrated significant lone-pair geometry effects on vicinal C−H bond lengths and strengths.[2,3,5,7,47] We propose that the shielding differences observed in the NMR studies are due to a hyperconjugative cause at CH1 and CH2 but not CH3 or CH5. For the latter protons, we suggest that the increased polarity toward carbon in the α-anomer is the result of electronic repulsion by the electron-rich axial oxygen.

Summary. A summary of the anomeric equilibrium effects is given in Table 6. Excluding the <1 kcal/mol anomeric difference in the antiperiplanar partner, the only effect experienced at H2 is the preferential orientation of OH2 at 60° in β-glucose and 160° in α-glucose. Scaling our results in 2-propanol to fit the experimental isotope effect of 1.027 implies the impact of this effect on both H1 and H3 to be 0.987.

(65) Bartell, L. S. *J.Am. Chem. Soc.* **1961**, *83*, 3567−71.
(66) Hruska, F. E.; Wood, D. J.; McCaig, T. N.; Smith, A. A.; Holy, H. *Can. J. Chem.* **1974**, *52*, 497−508.
(67) Dais, P.; Perlin, A. S. *Carbohyd. Res.* **1987**, *169*, 159−169.
(68) Gawlita, E.; Lantz, M.; Paneth, P.; Bell, A.; Tonge, P.; Anderson, V. *J. Am. Chem. Soc.* **2000**, *122*, 11660−11669.
(69) Grutzner, J. B.; Jautelat, M.; Dence, J. B.; Smith, R. A.; Roberts, J. D. *J. Am. Chem. Soc.* **1970**, *92*, 7107−20.
(70) Rao, V. S.; Perlin, A. S. *Carbohyd. Res.* **1981**, *22*, 141−8.
(71) Forrest, T. P.; Webb, J. G. K. *Org. Magn. Reson.* **1979**, *12*, 371−5.
(72) Lambert, J. B.; Vagenas, A. R. *Org. Magn. Reson.* **1981**, *17*, 270−7.
(73) Eliel, E. L.; Bailey, W. F.; Kopp, L. D.; Willer, R. L.; Grant, D. M.; Bertrand, R.; Christensen, K. A.; Dalling, D. K.; Duch, M. W.; Wenkert, E.; Schell, F. M.; Cochran, D. W. *J. Am. Chem. Soc.* **1975**, *97*, 322−30.
(74) Wiberg, K. B.; Barth, D. E.; Pratt, W. E. *J. Am. Chem. Soc.* **1977**, *99*, 4286−9.

Table 6. Summary of Contributors to Isotope Effects in Glucose

	phenomenon and effect							
H	anomeric effect	hydroxyl freezing	steric repulsion	antiperiplanar	solvation difference	γ-subst. effect	CH_2 restriction	total
1	1.100	0.987		0.961	?			1.043
2		1.027		1.000	?			1.027
3		0.987	1.025	1.010		1.000		1.022
4								1.000
5			1.025	1.010		1.000		1.035
6							1.000	1.000

Assuming that these phenomena combine as products in isotope effects, the intrinsic isotope effect at H1 due to a combination of a normal isotope effect caused by overlap with the p-type lone pair of O5 and an inverse isotope effect due to loss in antiperiplanar partners would have to be 1.057. On the basis of the NBO analysis and the isotope effect at H2, estimating the isotope effect per kcal/mol at 1% would give a 10% normal isotope effect at H1 due to the 10 kcal/mol advantage of p-type lone pair overlap and an inverse 3.9% effect due to the loss in antiperiplanar partner for that bond. A roughly 3.5% combined isotope effect due to steric restriction of angle bending modes and minor electron delocalization at H3 and H5 would be required to give approximately the correct results at these positions. We estimate the antiperiplanar hyperconjugation at approximately 10% of the anomeric effect due to our NBO analysis of the glucose anomers, leaving an isotope effect of 1.025 due to the steric repulsion of the axial 1-hydroxyl in α-glucose. The γ-substituent effect plays no role at H3 and H5, but a difference in solvation is certainly very likely to have some effect nearest the anomeric center. While the magnetic nonequivalence of the H6-pro*R* and H6-pro*S* methylene protons implies restricted motion and intramolecular interactions, these are apparently unchanged by anomeric configuration and do not give an observed isotope effect. We do not rule out solvation difference as a possible contributor. It seems most likely to play a role at OH1 and OH2, but presently the magnitude or direction of its contribution has not been assessed.

Other Isotope Effect Studies. The equilibrium isotope effects with glucose are necessary to interpret enzymatic kinetic isotope effects in terms of modeling transition state structure and for studies of equilibrium isotope effects in enzyme−ligand binding equilibria. Our demonstration of significant anomeric equilibrium isotope effects raises the possibility that solution conformers which do not undergo chemical transformation during reaction studies or do not participate in binding reactions may seriously bias observed isotope effects. This is of particular concern in studies of secondary ^{3}H-kinetic isotope effects since the anomeric effects observed here are similar in magnitude to those expected in kinetic studies. Tritium binding isotope effect studies may be similarly affected, as they depend on the magnitude of the equilibrium isotope effect, the equilibrium constant itself, and the relative binding affinities of the various solution conformers. The values reported here permit investigators to provide corrections for equilibrium deuterium or tritium isotope effects on glucose interactions with proteins.

Conclusion

We have found significant conformational equilibrium isotope effects on the anomeric equilibrium constant for glucose in aqueous solution. The results provide correction factors for the use of isotope effects to probe transition states and enzyme−ligand binding reactions. We have also been able to draw from the gas-phase calculations some conclusions about the energetics and conformations of glucose and the interplay of phenomena underlying conformational equilibrium isotope effects. Four of seven protons experience a less vibrationally constrained environment in β-glucose; two of these, H1 and H2, may be explained in hyperconjugative terms and two, H3 and H5, require some combination of steric repulsion and hyperconjugation. We consider the application of natural bond orbital analysis to a whole-molecule isotope effect study to be a significant advance toward understanding the forces which determine molecular structure.

Acknowledgment. We would like to express thanks to Drs. Sean Cahill and Mark Girvin for their important assistance with practical aspects of the ^{13}C NMR studies and Dr. Frank Weinhold for advice regarding NBO analysis.

Supporting Information Available: Natural bond orbital analysis of electron delocalization with a cutoff value of 0.9 kcal/mol, fractionation factors and calculations of ensemble isotope effects, and the geometries of minimized glucose models. This material is available free of charge via the Internet at http://pubs.acs.org.

JA003291K